II－78

INVESTIGATION OF TURBULENT BOUNDARY LAYER UNDER NON-LINEAR WAVES MOTION

Tohoku University Student Member, Graduate Student SUNTOYO
Tohoku University Fellow Member Hitoshi TANAKA

1. INTRODUCTION

The shape of the near-bed wave orbital velocity is a key parameter for cross-shore sediment transport under breaking and near-breaking waves. Ocean waves, in nature often have a strong non-linear shape related to the lack of horizontal and vertical symmetry known as the skew and asymmetric wave, respectively. It is though that wave boundary layer, bottom shear stress and sediment transport behaviors actualizing the effect of acceleration along the asymmetric and the skewness of wave is different from sinusoidal wave. Therefore, it is generally believed that the asymmetric and skew wave can cause a net cross-shore transport of sediment.

In the present paper, a rough turbulent boundary layer behaviors under cnoidal wave as representative of non-linear wave including mean velocity profile, turbulent intensity, bottom shear stress and turbulence kinetic energy budget were investigated through both the experimental and a two-layer baseline (BSL) k-ω turbulence model. Moreover, a new calculation method of bottom shear stress based on incorporating velocity and acceleration terms as proposed by Suntoyo et al. (2006), is used to examine the others calculation method, numerical model and the experimental results of bottom shear stress under non-linear wave.

2. EXPERIMENTAL STUDY

Rough turbulent flow experiments under cnoidal wave as representative of non-linear wave were carried out in an oscillating tunnel using air as the working fluid. The velocity was measured in the center part of wind tunnel at 20 points in the vertical direction by means of LDV. Triangular elements of roughness were chosen in order to the roughness elements protrude out of the viscous sub-layer. Thus, the velocity distribution near a rough bed is logarithmic. It can be therefore assumed that log-law can be used to estimate bottom shear stress over rough bed turbulent flow.

The experimental conditions are given in **Table 1**. The definition sketch for non-linear wave is shown in **Fig. 1**. Here, a_m/k_s is the roughness parameter, k_s is the Nikuradse's roughness equivalent defined as $k_s=30z_o$ in which z_o is the roughness height. T is wave period, t_p is time interval measured from the zero-up cross point to wave crest in the time variation of free stream velocity and $a_m=U_{max}/\sigma$, where, U_{max} is the velocity at wave crest, α is the wave skewness parameter, $N_i=U_{max}/\hat{u}$ is the non-linearity index and $\hat{u}$ is the total velocity amplitude. The smaller α and the higher N_i indicate more remarkable wave skewness and non-linearity, respectively. While the symmetric wave without skewness and non-linearity has N_i=0.50 and α=0.50.

Table 1 Experimental conditions

Case	T(s)	U_{max}(cm/s)	R_e	a_m/k_s	a	N_i
1	3.00	363	4.34 x10^5	115.6	0.393	0.67
2	3.00	360	4.27 x10^5	114.6	0.447	0.60
3	3.00	352	4.08 x10^5	112.0	0.457	0.58

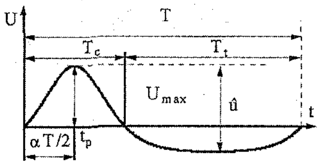

Fig. 1: Definition sketch for non-linear wave

3. NUMERICAL MODEL

In the present study, a two-layer k-ω model called as the baseline (BSL) k-ω model as proposed by Menter (1994) was used to clarify turbulent boundary layer properties of experimental result. The turbulence kinetic energy, k and the specific dissipation rate, ω, are obtained from the following transport equations,

$$\frac{\partial k}{\partial t}=\frac{\partial}{\partial z}\left\{\left(\nu+\nu_t\sigma_{k\omega}\right)\frac{\partial k}{\partial z}\right\}+\nu_t\left(\frac{\partial u}{\partial z}\right)^2-\beta^*\omega k \qquad (1)$$

$$\frac{\partial \omega}{\partial t}=\frac{\partial}{\partial z}\left\{\left(\nu+\nu_t\sigma_{\omega}\right)\frac{\partial \omega}{\partial z}\right\}+\gamma\frac{\nu+\nu_t}{\nu_t}\left(\frac{\partial u}{\partial z}\right)^2$$
$$-\beta\omega^2+2\left(1-F_1\right)\sigma_{\omega 2}\frac{1}{\omega}\frac{\partial k}{\partial z}\frac{\partial \omega}{\partial z} \qquad (2)$$

$$\nu_t=\frac{k}{\omega} \qquad (3)$$

where, $\sigma_{k\omega}$, β^*, σ_ω, γ and β are model constants, F_1 is a blending function. The left hand side of the k and ω equation specifies the rate of change. On the right hand side, the first term is the viscous and turbulent diffusion, second term is the production of turbulent kinetic energy and specific dissipation and the last term specifies the dissipation of turbulence and dissipation of the dissipation.

The boundary condition at the wall which is used are no-slip boundary condition for velocities and turbulent kinetic energy, i.e. at z = 0, u = k =0, and at the axis of symmetry of the oscillating tunnel, the gradients of velocity, turbulent kinetic energy and specific dissipation rate are equal to zero, i.e. at $z=z_h$, $\partial u/\partial z=\partial k/\partial z=\partial\omega/\partial z=0$. Effect of roughness was introduced through the wall boundary condition as proposed by Wilcox (1998). Numerical method explanation can be found in detail in Suntoyo et al. (2006).

4. RESULTS AND DISCUSSION

Mean velocity profiles in the rough turbulent boundary layer for cnoidal waves at selected phases were compared with the BSL numerical model as shown in **Figs. 2**. The solid line showed the BSL k-ω model while open and closed circles (○ and ●) showed the experimental results of mean velocity profile distribution. As seen that both for experimental and the BSL k-ω model results, the velocity overshoot is much influenced by the effect of acceleration and the velocity magnitude. The velocity overshoot at phases of B, C and D are higher than that of at phases of F, G and H. The velocity profiles of experimental results showed a good agreement with the BSL k-ω model prediction at the phases of B, C, especially where the velocity overshooting occurs. During the deceleration phases where the pressure gradient is not so steep as in the present asymmetric wave cases, it seem that the BSL k-ω model slightly fails to cope with the flow situation.

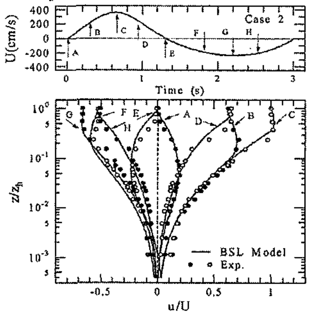

Fig. 2 Mean velocity profiles for Case 2 with $N_i = 0.60$

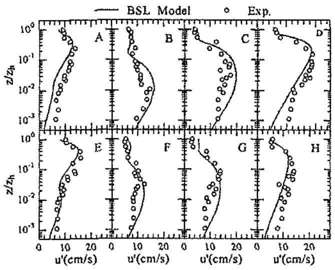

Fig. 3 Turbulent intensity profiles for Case 2 with $N_i = 0.60$

The turbulent intensity or the fluctuating velocity in x direction, u' can be computed using Eq. (4) as proposed by Nezu (1977) from the turbulent kinetic energy provided in the BSL k-ω model.

$$u' = 1.052\sqrt{k} \tag{4}$$

Comparison of BSL k-ω model prediction and experimental data of turbulent intensity at selected phases for Case 2 is shown in **Fig. 3**. The turbulent intensity almost uniformly distributed across the depth, where the free - stream velocity is zero, namely at phases of A and E. Moreover, higher turbulent intensity close to the bottom occurs at C and G phases due to the higher mean velocity at crest and trough of wave. An excellent agreement is shown across the depth at the phase of E. The model prediction far from the bed is generally good, while near the bed is not so much in good agreement.

Fig 4 shows the turbulent kinetic energy budget of k across the boundary layer at phase B and D for case 2. During acceleration phase at phase B the model has been able to produce almost balance for turbulent production, turbulent dissipation and turbulent diffusion, so that the velocity profile is very well in agreement with the experimental data at the phase B as shown in **Fig. 2**. While during deceleration phase at phase D, the value of production term is greater far from the value of dissipation term and the sum of all the term (imbalance) can be not almost zero. As seen in **Fig. 2** that a good agreement of mean velocity between the model and experiment results could not be obtained at the phase D.

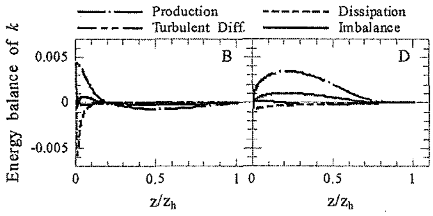

Fig. 4 Turbulent kinetic energy budget of k for Case 2

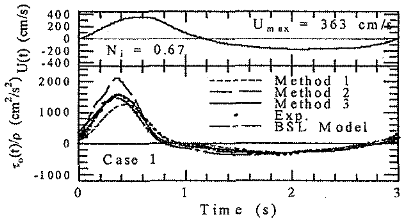

Fig. 5 Time-variation of bottom shear stress for Case 1

Bottom shear stress of experimental result is examined with two existing calculation methods (Method 1 and Method 2), BSL k-ω model and the new method (Method 3) as proposed by Suntoyo et al. (2006). Method 3 has given the best agreement with the experimental result along a wave cycle as shown in **Fig. 5**, while Method 1 gave under estimate value of bottom shear stress especially at crest part caused by incorporating the acceleration term was not done in Method 1. It is confirmed that the acceleration effect has significant role in the calculation of bottom shear stress under cnoidal waves. Method 2 was not a reliable method for calculating the bottom shear stress under cnoidal waves, though the acceleration terms has been included for calculating. Moreover, the BSL model prediction result showed more close to both the experimental result and Method 3. Due to wave non-linearity, the wave-induced the bottom shear stress distribution is characterized by a large peak over a very short time interval preceding the wave crest. These characteristics are much more obvious for the higher non-linear wave case. As seen that Case 1 produced a largest peak over shortest time interval preceding the wave crest than others cases.

5. CONCLUSIONS

The behaviors of the rough turbulent boundary layer under non-linear wave has been examined through both experimental and BSL k-ω model. Moreover, the new method of bottom shear stress under non-linear wave can be further used to an input sediment transport model under rapid acceleration in practical application on near-shore.

REFERENCES

Menter, F. R.: Two-equation eddy-viscosity turbulence models for engineering applications, *AIAA Journal*, Vol. 32, No. 8, pp. 1598-1605, 1994.

Nezu, I.: *Turbulent structure in open channel flow*, Ph.D. Dissertation, Kyoto University, Japan, 1977. (in Japanese)

Suntoyo, Tanaka, H., Sana, A. and Yamaji, H.: Characteristics of turbulent boundary layer over a rough bed under cnoidal waves motion, *Annual Journal of Hydraulic Eng*, JSCE, Vol. 50, 2006.

Wilcox, D.C.: Reassessment of the scale-determining equation for advanced turbulent models, *AIAA Journal* Vol. 26, No. 11, pp. 1299-1310, 1988.